














Ulinastatin alleviates early brain injury after intracerebral hemorrhage by inhibiting necroptosis and neuroinflammation via MAPK/NF- κ B signaling pathway

Li Wang¹ , Wei Jiao² , Jiayu Wu³ , Jing Zhang⁴ , Min Tang³ , Yang Chen^{5*} 

1. BS. Anhui Medical University  – Wuxi Clinical College – 904th Hospital of Joint Logistic Support Force of PLA – Department of Neurology – Wuxi, China.
2. BS. Anhui Medical University  – Wuxi Clinical College – 904th Hospital of Joint Logistic Support Force of PLA – Department of Nursing – Wuxi, China.
3. MM. Anhui Medical University  – Wuxi Clinical College – 904th Hospital of Joint Logistic Support Force of PLA – Department of Neurology – Wuxi, China.
4. MM. Anhui Medical University  – Wuxi Clinical College – 904th Hospital of Joint Logistic Support Force of PLA – Department of Nursing – Wuxi, China.
5. MD. Anhui Medical University  – Wuxi Clinical College – 904th Hospital of Joint Logistic Support Force of PLA – Department of Neurology – Wuxi, China.

ABSTRACT

Purpose: Spontaneous intracerebral hemorrhage (ICH) is a major public health problem with a huge economic burden worldwide. Ulinastatin (UTI), a serine protease inhibitor, has been reported to be anti-inflammatory, immune regulation, and organ protection by reducing reactive oxygen species production, and inflammation. Necroptosis is a programmed cell death mechanism that plays a vital role in neuronal cell death after ICH. However, the neuroprotection of UTI in ICH has not been confirmed, and the potential mechanism is unclear. The present study aimed to investigate the neuroprotection and potential molecular mechanisms of UTI in ICH-induced EBI in a C57BL/6 mouse model. **Methods:** The neurological score, brain water content, neuroinflammatory cytokine levels, and neuronal damage were evaluated. The anti-inflammation effectiveness of UTI in ICH patients also was evaluated. **Results:** UTI treatment markedly increased the neurological score, alleviate the brain edema, decreased the inflammatory cytokine TNF- α , interleukin-1 β (IL-1 β), IL-6, NF- κ B levels, and RIP1/RIP3, which indicated that UTI-mediated inhibition of neuroinflammation, and necroptosis alleviated neuronal damage after ICH. UTI also can decrease the inflammatory cytokine of ICH patients. The neuroprotective capacity of UTI is partly dependent on the MAPK/NF- κ B signaling pathway. **Conclusion:** UTI improves neurological outcomes in mice and reduces neuronal death by protecting against neural neuroinflammation, and necroptosis.

Key words: Cerebral Hemorrhage. Stroke. Brain Injuries. Necrosis. RIP1/RIP3.

*Correspondence author: wg2010@21cn.com | +86 (510) 85142114

Received: Nov 16, 2021 | Review: Jan 13, 2022 | Accepted: Feb 14, 2022

Conflict of interest: Nothing to declare.

Research performed at Department of Neurology, 904th Hospital of Joint Logistic Support Force of PLA, Wuxi Clinical College of Anhui Medical University, Wuxi, China.



■ Introduction

Spontaneous intracerebral hemorrhage (ICH) has the highest mortality rate among stroke subtypes, accounts for 15% to 20% of all stroke types, and has an increased incidence in elderly patients¹⁻⁴. Acute ICH due to a large intracranial hematoma is associated with high morbidity and mortality, as it can lead to primary brain injury through the destruction of brain tissue and the high intracranial pressure (ICP) that results from the large hematoma^{5,6}. Previous studies revealed that craniotomy for hematoma evacuation is an effective therapy for limiting primary brain damage and decreasing ICP after ICH, which is of substantial interest⁶⁻⁸. However, craniotomy for hematoma evacuation shows no clinical benefit to patients, no improvement in long-term outcomes, and rarely affects neurological recovery⁹. Increasing evidence shows that red blood cell debris, hemoglobin, its degradation products, and blood components trigger secondary brain injury following ICH and contribute to a series of damaging events, including neuroinflammation, brain edema, oxidative stress, blood-brain barrier (BBB) damage, and neuron death¹⁰⁻¹², which can be reversed^{13,14}. According to the previous studies¹⁵⁻¹⁷, inhibition of oxidative stress, decreases mitochondrial apoptosis, can improve neurological function, and decreases cerebral edema after ICH in mice. Currently, the neuroprotective effect of the inhibition of necroptosis and neuroinflammation remains unclear.

Ulinastatin (UTI) is a serine protease inhibitor with a molecular weight of 67,000 purified from human urine. The main pharmacological activities of UTI were anti-inflammatory, immune regulation, and organ protection^{18,19}. A drug widely used to treat acute inflammatory disorders such as sepsis, ischemia-reperfusion injury, and antiapoptotic actions²⁰. He²¹ reported that UTI may be of value for the inhibition of postoperative increased inflammatory agents and most likely provided pulmonary protective effects in cardiac surgery by meta-analysis of 15 randomized controlled trials. Additionally, in recent studies with animals, UTI had been reported that can alleviate early brain injury, cerebral ischemia-reperfusion injury, and permeability of the blood-brain barrier in the animal transient middle cerebral artery occlusion (tMCAO) model²²⁻²⁴. However, the effects of UTI on the EBI in the acute phase of ICH are not clear, and their association with levels of apoptotic molecules and oxidative stress remains to be elucidated.

Necroptosis is a newly discovered pathway of regulated necrosis, a caspase-independent programmed cell death mechanism that requires the proteins RIPK3 and MLKL and is induced by death receptors²⁵. Increasing evidence suggests that necroptosis plays a critical role in central nervous system diseases, including traumatic brain injury²⁶⁻²⁸, ICH^{29,30}, ischemic stroke³¹, amyotrophic lateral sclerosis, Parkinson's disease, and Alzheimer's disease³². The most upstream signaling activity required for the induction of necroptosis is the activation of a TNF ligand family member (e.g., protein kinase function of receptor-interacting protein kinase-1 [RIPK1] and mixed lineage kinase domain-like [MLKL]); RIPK1 activation leads to necroptosis through the formation of a RIPK1-RIPK3-MLKL complex³³. Zhang³⁴ also reported that selenium can prevent necroptosis by restoring antioxidant functions and blocking the MAPK/NF- κ B pathway in the chicken spleen. Necroptosis is common in early brain injury³⁵ and may be an effective mechanism of ICH.

In the present study, a mouse ICH model was constructed to study the effects of UTI on EBI and explored the crosstalk between oxidative stress and neuroinflammation. The mechanism by which the MAPK/NF- κ B signaling pathway may regulate this process was also explored.

■ Methods

All animal experiments performed in this study complied with the National Institutes of Health guidelines for the handling of laboratory animals and were approved by the Ethics Committee of the Wuxi Medical College of Anhui Medical University (YXLL-2020-049).

Animal ICH model

A total of 45 healthy adult C57BL/6J mice were randomly assigned to the Sham group, SAH group, and SAH+UTI group. All experiments were conducted on healthy adult male C57BL/6J mice (22–25 g) (Anhui Medical University, Hefei, China). The mice were housed in animal care facilities on a 12 h light/dark cycle and had free access to food and water.

The ICH mouse model was generated based on a previously described protocol involving autologous blood injection³⁶. Briefly, male C57BL/6J mice were anesthetized by intraperitoneal injection of 50 mg·kg⁻¹ pentobarbital sodium and placed in a prone position with a stereotactic head frame. The rectal temperature was kept at 37 ± 0.5 °C during the operation using a heating pad. An artificial tear ointment was used to protect the eye from injury during surgery. A midline scalp incision was made, and a cranial burr hole with a 1-mm diameter was made at the following coordinates relative to bregma: 0.2 mm posterior, 2.2 mm lateral to bregma, and 3.5 mm below the dura. A total of 30 µL of autologous blood without anticoagulation was collected from the caudal artery and rapidly injected into the basal ganglia through the burr hole via the 26-gauge needle of a 10-µL Hamilton syringe. First, 5 µL of arterial blood was injected at a depth of 2.8 mm from the dura (injection speed: 3 µL·min⁻¹). Five minutes later, the other 25 µL of blood was injected at a depth of 3.5 mm (injection speed: 3 µL·min⁻¹). After the injection of autologous blood, the needle was kept in the brain for 10 min to prevent blood backflow along the needle tract. Finally, the hole was covered with medical bone wax. The animals in the Sham group received similar surgical procedures but were injected at the same site with an equal volume of sterile saline instead of blood.

Drug administration

The UTI (Techpool Biochem, Guangdong, China) was stored at 4 °C and dissolved in 0.9% normal saline when it is used. A 10⁴ U·kg⁻¹ UTI was administered by intraperitoneal injection before the onset of ICH²⁰.

Neurobehavioral assessment

The severity of brain injury was evaluated by determining neurological function 72 h after ICH using a previously described neurological grading system³⁷. The scoring system consisted of motor, sensory, reflex, and balance tests. The neurological scores ranged from 0 to 18 points and were calculated by adding the scores together; all mice in each group underwent a behavioral assessment, and a higher score represented worse neurological function. All mouse behavior scores were recorded by the same independent observer who was blinded to the study groups.

Brain water content measurement

The severity of brain edema was evaluated by measuring the brain water content using the standard wet-dry method, as previously reported³⁸⁻⁴⁰. The mice were sacrificed 72 h after ICH, and the entire brain was harvested and separated into the ipsilateral and contralateral cortices, ipsilateral and contralateral basal ganglia, and cerebellum (wet weight). Then, brain specimens from each group were dehydrated at 105 °C for 24 h to acquire the dry weight. The percentage of brain water content was equal to (wet weight – dry weight)/wet weight × 100%.

Evans blue extravasation

Evans blue extravasation was performed as previously described⁴¹. Briefly, mice were anesthetized by pentobarbital sodium (50 mg·kg⁻¹) injection 48 h after ICH. Evans blue dye (2%, 5 mL·kg⁻¹; Sigma–Aldrich, St. Louis, MO, USA) was injected into the left femoral vein over 2 min and circulated for 60 min. Then, the mice were sacrificed with 100 mg·kg⁻¹ sodium pentobarbital via intraperitoneal injection and with phosphate-buffered saline (PBS) intracardial perfusion. The brains were removed and quickly divided into the left and right cerebral hemispheres, weighed, homogenized in saline, and centrifuged at 15,000 g for 30 min. Subsequently, the resultant supernatant was added with an equal volume of trichloroacetic acid, incubated overnight at 4 °C, and centrifuged at 15,000 g for 30 min. Next, the resultant supernatant was collected and spectrophotometrically quantified at 610 nm for Evans blue dye.

Cytokine measurements

The ipsilateral cortex tissue in animals and ICH patients' serum were collected and detected. The levels of IL-1β (cat. No. ab197742; Abcam), IL-6 (cat. No. ab222503; Abcam), TNF-α (cat. No. ab208348; Abcam), and NF-κB

(cat. No. ab176663; Abcam) were measured by the enzyme-linked immunosorbent assay (ELISA), according to the manufacturer's instructions.

TUNEL staining

A TUNEL assay was conducted to assess neuronal death in the hippocampus. The TUNEL reaction mixture (50 μ L) was added to each sample, and the slides were incubated in a humidified chamber for 60 min at 37 °C in the dark. The slides were then incubated with DAPI for 5 min at room temperature in the dark to stain the nuclei, followed by imaging with a fluorescence microscope. The procedure was performed with a TUNEL staining kit according to the manufacturer's instructions. A negative control (without the TUNEL reaction mixture) was used. The cell count was confirmed in four randomly selected high-power fields, and the data obtained from each field were averaged.

Western blot analysis

Western blot analyses were performed as previously described³⁸. Briefly, cerebral cortex samples were collected, homogenized, and separated by sodium dodecyl sulfate-polyacrylamide gel electrophoresis on 10% polyacrylamide gels. A BCA Protein Assay Kit (Beyotime) was used to measure protein concentrations with the bicinchoninic acid method. After separation, protein samples were transferred onto immobilon nitrocellulose membranes. The membranes were blocked with 5% nonfat milk at room temperature for 1 h. The membranes were then incubated with the following primary antibodies overnight at 4 °C: rabbit anti- β -actin (1:1000, rabbit polyclonal, Abcam, ab8227), rabbit anti-RIP1 (1:1,000; rabbit polyclonal; Abcam; cat. No. ab106393), rabbit anti-RIP3 (1:1,000; rabbit polyclonal; Abcam; cat. No. ab62344), phospho-p38 (CST, No. 4551, 1:2000), rabbit anti-NF- κ B (1:1000, rabbit monoclonal, Abcam, ab32360). After washing the membranes with TBST three times, HRP-conjugated goat antirabbit IgG or goat antimouse IgG secondary antibodies (1:5000) were applied, and the membranes were incubated with the secondary antibodies at room temperature for 1.5 h. The protein bands were detected using a Bio-Rad imaging system (Bio-Rad, Hercules, CA, USA) and quantified with ImageJ software.

Quantitative real-time polymerase chain reaction (PCR)

Quantitative real-time PCR analysis was performed as previously indicated⁴². Total RNA was extracted from either cell cultures or hippocampal brain samples using TRIzol Reagent (Gibco; Thermo Fisher Scientific, Inc., Waltham, MA, USA) according to the manufacturer's instructions. Then, RNA was reverse transcribed to complementary DNA (cDNA) using the RevertAid First Strand cDNA Synthesis Kit (K1622; Thermo Fisher Scientific Inc., Rockford, IL). MAPK and Nrf2 mRNA levels in each sample were measured by qPCR using SYBR Green Master Mix (Toyobo Co., Ltd., Osaka, Japan). GAPDH was used as an internal control. The qPCR thermocycling conditions were as follows: 45 °C (2 min) and 95 °C (10 min), followed by 40 cycles of denaturation at 95 °C (15 s), annealing at 60 °C (1 min), and extension at 72 °C (1 min). All samples were analyzed in triplicate. The target genes and the specific primers are the following:

NF- κ B (forward, 5'- ATCACGAGCCCTGAAACCAA-3'; reverse, 5'-GGCTGCAAAATGCTGGAAAA-3'),

MAPK (forward, 5'- TGTGTTACCCCTGCCAAGT-3'; reverse, 5'-GCCCCGAAGAATCTGGTAT-3')

GAPDH (forward, 5'- ATGGGTGTGAACCACGAGA-3' and reverse, 5'-CAGGGATGATGTTCTGGGCA-3')

Statistical analysis

The data are reported as the means and standard deviation (SD). The SPSS 14.0 (SPSS, Chicago, IL, USA) and GraphPad Prism 6 (GraphPad Software, San Diego, CA, USA) softwares were used for the statistical analyses. Student's t-test was used if two groups were compared, and one-way analysis of variance (ANOVA) followed by Bonferroni's post hoc test were used if two independent variables were compared. For all statistical analyses, differences were considered significant at $p < 0.05$.

Results

UTI alleviates neurological deficits and mortality after ICH

The effect of UTI treatment on long-term neurological damage parameters was evaluated including mortality rates and neurological scores. As shown in Fig. 1, mortality rates (Fig. 1a) and neurological score (Fig. 1b) in various groups, including Sham, ICH, ICH + UTI. ICH significantly increased the mortality rates. It was alleviated by the UTI treatment, while no significant difference. Similar results were obtained for neurological scores, which were decreased significantly after ICH, and UTI administration significantly improved neurological function.

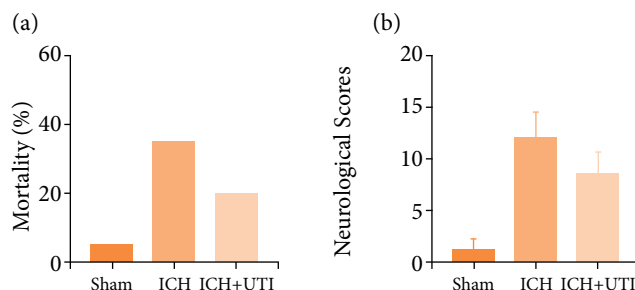


Figure 1 - UTI alleviates neurological deficits and mortality after ICH. (a) Comparison of the mortality between the three groups, the mortality increased significantly after ICH, Mortality rates in the Sham group (5%), ICH group rate (35%), the ICH + UTI group rate (15%); (b) Neurological scores of mice in the sham group, ICH group, and ICH group treated with UTI at 72 h (n = 10, *p < 0.05 vs. Sham; #p < 0.05 vs. ICH; ANOVA; means \pm SD).

UTI alleviate brain edema and BBB permeability after ICH

To clarify the EBI after ICH, brain water content by the wet-dry method at 72 h after ICH was used to evaluate brain damage. The results showed that ICH increased the brain water content significantly, which was alleviated after UTI treatment (Fig. 2a). Similar results in BBB permeability, which were increased significantly after ICH, and UTI administration can significantly alleviate (Fig. 2b). Hence, UTI treatment markedly improves BBB permeability and alleviated brain edema at 72 h.

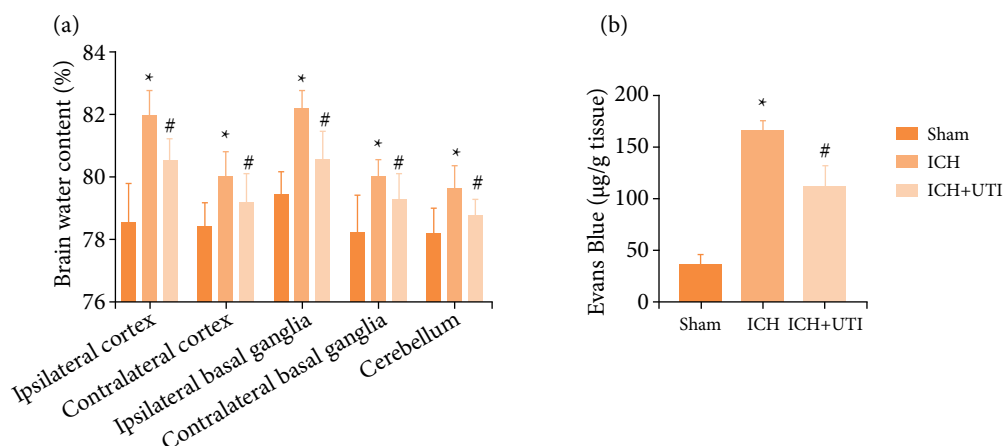


Figure 2 - UTI alleviate brain edema and BBB permeability after ICH. (a) UTI alleviates brain water content after ICH; (b) UTI alleviates BBB permeability after ICH (n = 5, *p < 0.05 vs. Sham; #p < 0.05 vs. ICH; ANOVA; means \pm SD).

UTI alleviates neuronal necroptosis after ICH

TUNEL assay was used to evaluate the level of cell death in ICH mice treated with and without UTI at 72 h after model construction. The results revealed more hippocampal neuronal death after ICH, and UTI decreased neuronal apoptosis (Fig. 3). Based on these results, UTI exerts neuroprotective effects after ICH. The expression levels of necroptosis-related protein were detected by western blotting (Fig. 3b). The results of western blotting also indicated that UTI can reduce the expression levels of necroptosis-related protein RIP1 and RIP3 (Fig. 3 c-d). These results demonstrate that UTI has neuroprotective effects after ICH.

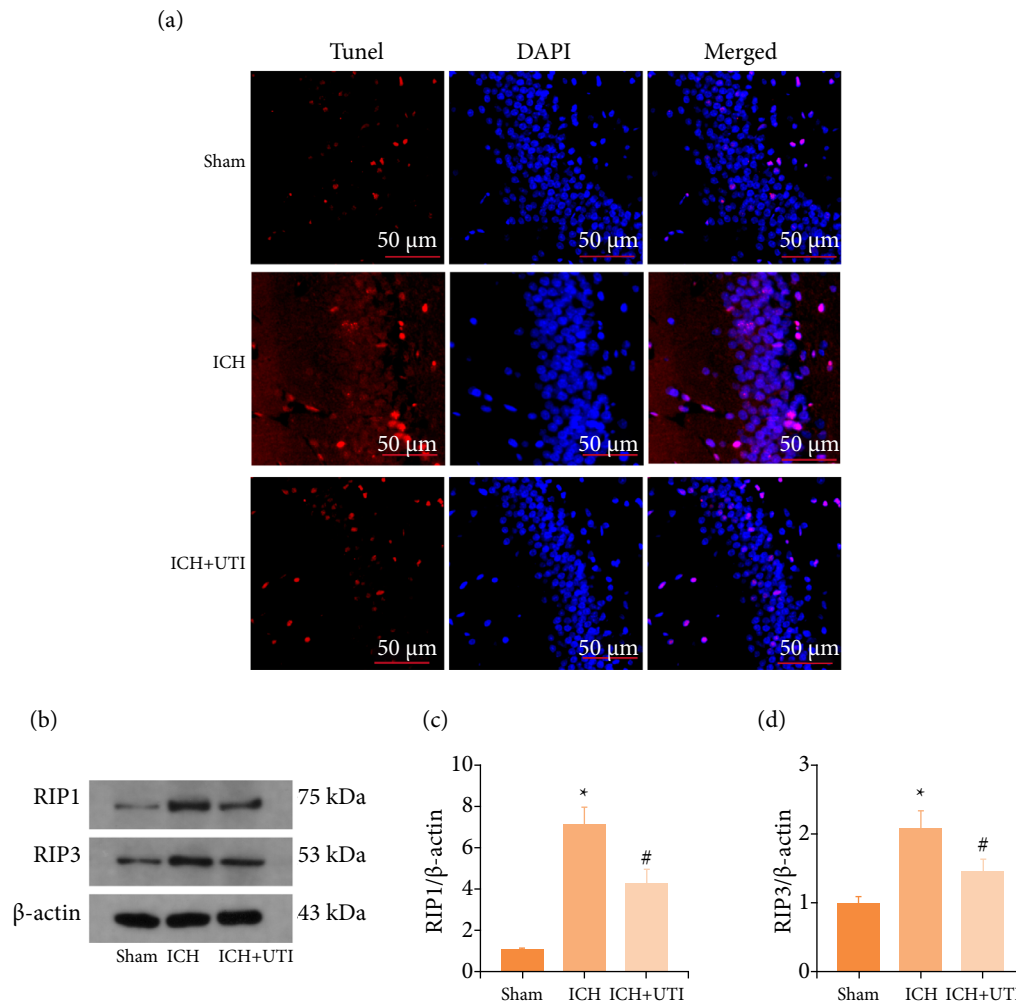


Figure 3 - UTI alleviates neuronal necroptosis after ICH. **(a)** TUNEL staining showed that UTI alleviated neuronal apoptosis in the hippocampus at 72 h after ICH, and representative images of apoptotic neurons are shown. Scale bar = 50 μ m; **(b)** Levels of RIP1 and RIP3 in the brain cortex of mice after TBI were determined using Western blotting; **(c)** Quantification of RIP1 levels in the brain cortex relative to β -actin, the loading control; **(d)** Quantification of RIP3 levels in the brain cortex relative to β -actin. DAPI, 4',6-diamidino-2-phenylindole; SAH, subarachnoid hemorrhage; TUNEL, terminal deoxynucleotidyl transferase dUTP nick end labeling.

UTI alleviates neuroinflammation after ICH

As previous studies^{34,40} have identified a vital role for neuroinflammation in EBI after ICH, increased neuroinflammation aggravates EBI. The inflammatory complex induces the secretion of proinflammatory cytokines, including IL-1 β , IL-6, and

TNF- α , and the subsequent activation of proinflammatory signaling through NF- κ B to initiate pyroptosis. Therefore, the hippocampal levels of IL-1 β , IL-6, TNF- α , and NF- κ B were measured using ELISAs. The levels of the proinflammatory cytokines were increased significantly after ICH, while the levels of proinflammatory cytokines decreased significantly after UTI treatment (Fig. 4 a-d). Hence, these results suggested that UTI exhibited potent anti-inflammatory activity against ICH-induced neuroinflammation.

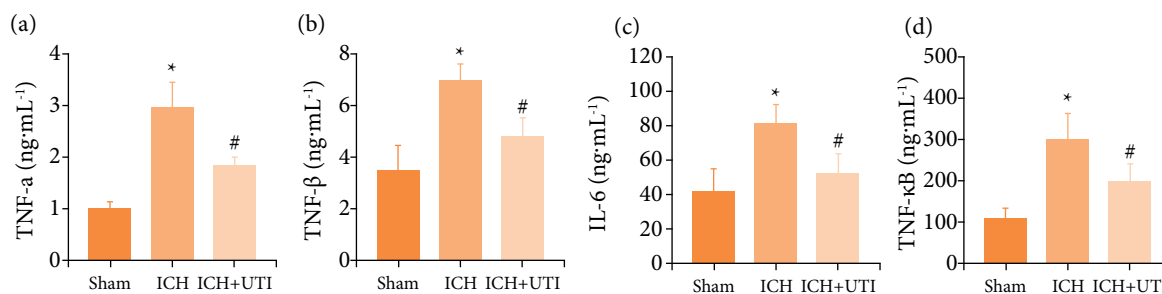


Figure 4 - UTI alleviates neuroinflammation after ICH. UTI significantly reduced hippocampal (a) TNF- α ; (b) interleukin-1 β (IL-1 β); (c) IL-6; and (d) NF- κ B levels at 72 h after ICH (n = 5, *p < 0.05 vs. Sham; # p < 0.05 vs. ICH, ANOVA; means \pm SD).

UTI regulates necroptosis and neuroinflammation by modulating the MAPK/NF- κ B signaling pathway after ICH

MAPK/NF- κ B was a core signaling pathway of necroptosis and neuroinflammation^{43,44}. Whether the neuroprotection of UTI regulates necroptosis and neuroinflammation was explored by modulating the MAPK/NF- κ B signaling pathway after ICH. The levels of the MAPK and NF- κ B protein were detected by performing western blotting (Fig. 5a). The levels of MAPK and NF- κ B were increased significantly in the ICH group and decreased after UTI administration (Fig. 5 b-c). Additionally, real-time PCR also demonstrated a similar result (Fig. 5 d-e). Thus, these results showed that neuroprotection of UTI may be by regulating the MAPK/ NF- κ B signaling pathway.

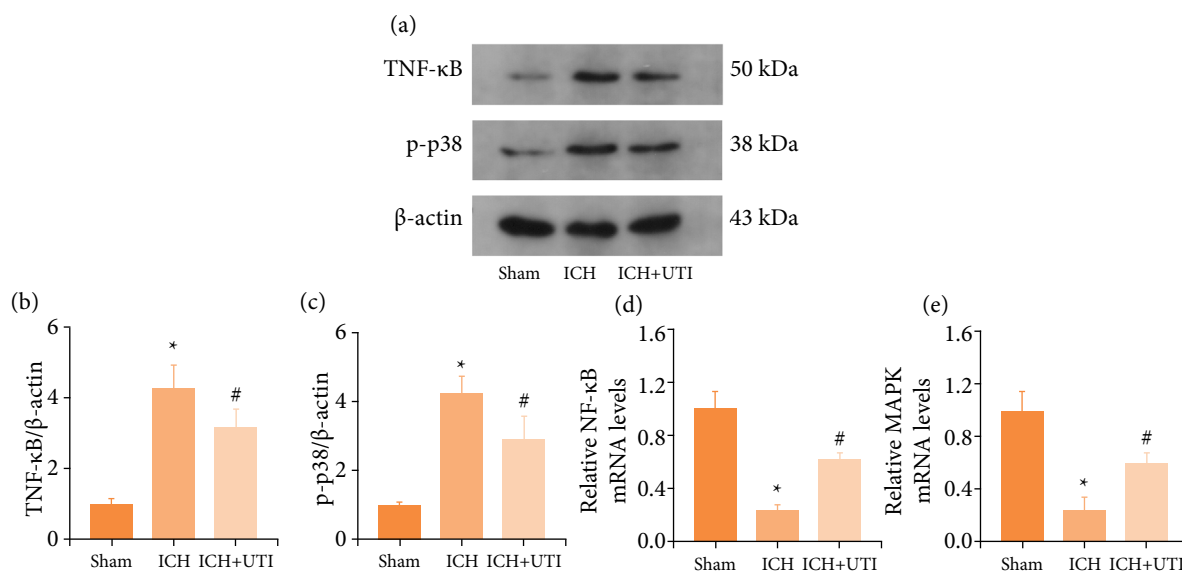


Figure 5 - UTI regulates necroptosis and neuroinflammation by modulating the MAPK/ NF- κ B signaling pathway after ICH. (a) Levels of MAPK, and NF- κ B in the brain cortex of mice after ICH were determined using Western blotting; (b) Quantification of NF- κ B levels in the brain cortex relative to β -actin, the loading control; (c) Quantification of MAPK levels in the brain cortex relative to β -actin; (d) Levels of NF- κ B mRNA in the brain of ICH mice were measured by real-time PCR; (e) Levels of MAPK mRNA in the brain of ICH mice were measured by real-time PCR (n = 5, Data are presented as the mean \pm SD, *p < 0.05 vs. Sham; #p < 0.05 vs. ICH).

UTI decrease the levels of the proinflammatory cytokine in ICH patients

To verify the antineuroinflammation in ICH patients, the expression levels of serum IL-1 β , IL-6, TNF- α , and NF- κ B in ICH patients were evaluated. The serum levels of IL-1 β , IL-6, TNF- α , and NF- κ B were measured using ELISAs. The levels of the proinflammatory cytokines were increased significantly after ICH, while the levels of proinflammatory cytokines decreased significantly after UTI treatment (Fig. 6 a, b), the results were similar to the animals.

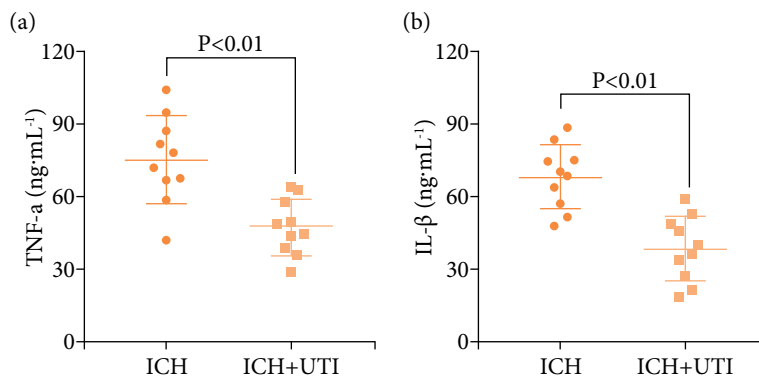


Figure 6 - UTI alleviates neuroinflammation in ICH patients. UTI significantly reduced ICH patients' serum (a) TNF- α ; (b) interleukin-1 β (IL-1 β) levels at 72 h after ICH (n = 10, p < 0.01, ANOVA; means \pm SD).

Discussion

Here, the therapeutic potential of UTI to alleviate early brain injury was evaluated in a mouse model of ICH. As shown in the present study, UTI is a neuroprotective agent that attenuates early brain injury following ICH. It showed that UTI (1) improves neurological dysfunction after ICH, (2) alleviates brain damage in a mouse ICH model, (3) relieves neuroinflammation after ICH and then decreases inflammatory damage in the brain, and (4) prevents necroptosis after ICH and alleviates neuronal death; (5) the antinecroptosis and antineuroinflammation effects of UTI may be related to the MAPK/NF- κ B signaling pathway (Fig. 7).

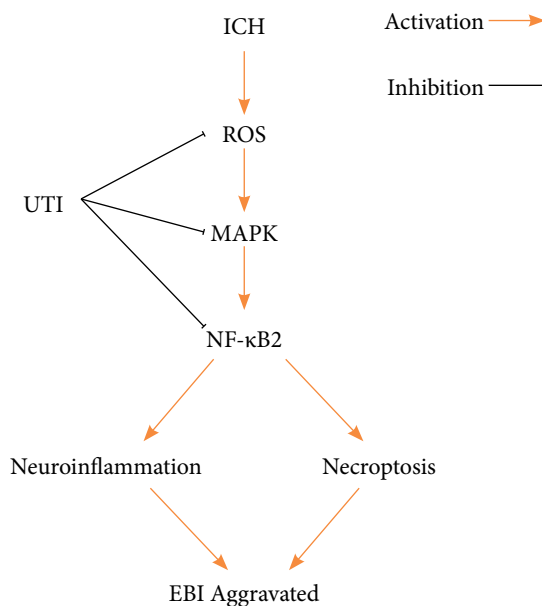


Figure 7 - A diagram of the proposed model explaining the observations of MAPK/NF- κ B -mediated regulation of necroptosis, and neuroinflammation after ICH and potential mechanisms underlying the effect of the UTI intervention.

UTI was a 67 kDa glycoprotein purified from the urine of healthy humans, nonspecific protease inhibitor, a urinary trypsin inhibitor, which was used to treat acute inflammatory disorders, sepsis, toxic shock, and hemorrhagic shock^{45,46}. Recent studies had demonstrated that UTI can alleviate cerebral ischemia-reperfusion injury by regulating inflammation and oxidative stress^{22,47}. However, the neuroprotection of UTI in ICH was unclear, and lacked related clinical studies. Liu¹⁹ reported that UTI can decrease the brain water content and blood-brain barrier permeability significantly after ICH, maybe through decreased activation of the astrocytes and ET-1, inhibited the expression of proinflammatory VEGF and MMP-9. Another study also reported that UTI can attenuate brain edema after male Sprague-Dawley rats ICH, the preliminary molecular mechanism may be through the decrease of the expression level of aquaporin-4 (AQP4), and proinflammatory cytokines including IL-1 β and TNF- α as well as activity of NF- κ B⁴⁸. The present study also demonstrated that UTI can alleviate brain edema, improve neurological function, relieve neuroinflammation response, and decrease hippocampal neuronal damage and necroptosis. Yang⁴⁹ reported that necroptosis and neuroinflammation were important mechanisms to lead EBI after ICH, and inhibition of these mechanisms can improve neurological outcomes, and reduce neuronal damage. Pan⁵⁰ also indicated that antinecrosis chemical necrostatin-1 can suppress apoptosis and autophagy in mice ICH model. Similar results were also demonstrated and the potential mechanism may be through RIP1/RIP3/MLKL pathway^{51,52}.

As the pharmacological action of UTI was more complex, included anti-inflammatory, immune regulation, and organ protection^{18,19}. The mechanism of neuroprotection of UTI after ICH also was multiple and complicated. Li²³ also demonstrated that UTI can protect the brain against ischemic injury, the potential molecular mechanism may be through to restore the BBB permeability by decreased expression of MMP-9 and increased ZO-1 and occludin proteins expressions. The mechanisms and molecules regulating necroptosis and neuroinflammation were very complex. The results in the present study, UTI also can decrease the expression levels of MAPK and NF- κ B, then alleviate the activation of necroptosis and neuroinflammation. Activated p38 MAPK could facilitate the disassociation of Nrf2 from Keap1 to initiate the transcription of several antinecrosis, antiapoptosis, and antioxidant genes, such as HO-1, quinone oxidoreductase-1 (NQO1), and glutathione peroxidase 4 (GPX4)^{6,53}. Li⁵⁴ also reported that UTI can improve neurological function, and alleviate brain edema and infarct volume by decreasing the expression of TLR4 and NF- κ B in the tMCAO model. Cui⁴⁸ also confirmed that the activity of IL-1 β , TNF- α , and NF- κ B was inhibited by UTI treatment in traumatic brain injury. ICH leads to intracellular reactive oxygen species accumulation and decreases the expression levels of TLR4, and the TLR4/NF- κ B/p65 signaling pathway also directly regulates neuroinflammation and necroptosis. In the present study, it was also observed that UTI can alleviate EBI after ICH through regulating crosstalk between oxidative stress and neuroinflammation, the potential mechanism may be mediated MAPK/NF- κ B signaling pathway. The specific mechanism remains unclear, and other potential molecular mechanisms may coexist and play a synergistic role. Therefore, further research is needed to explore these mechanisms. In addition, this experiment was performed in mice, and debate persists regarding whether the treatment is effective in humans. In the future, the clinical effect of UTI on patients with ICH will be further explored.

■ Conclusions

In summary, this study provided evidence that necroptosis and neuroinflammation are emerged as important cellular regulatory mechanisms, and contributed to EBI after ICH. In this study, the UTI-mediated regulation of necroptosis and neuroinflammation by the MAPK/NF- κ B pathway and provided a new idea to explore the biological effects and mechanisms underlying the antinecrosis, anti-inflammatory, and neuroprotective properties of UTI.

■ Authors' contribution

Design of the study: Wang L, Tang M and Chen Y; **Technical procedures:** Wang L, Jiao W, Wu J, Zhang J and Chen Y; **Manuscript writing:** Wang L; **Critical revision:** Wang L, Tang M and Chen Y; **Final approval the version to be published:** Wang L, Jiao W, Wu J, Zhang J, Tang M and Chen Y.

■ Data availability statement

All datasets were generated or analyzed in the current study.

■ Funding

Not applicable.

■ Acknowledgments

Not applicable.

■ References

1. Zhang Y, Zhang X, Wei Q, Leng S, Li C, Han B, Bai Y, Zhang H, Yao H. Activation of sigma-1 receptor enhanced pericyte survival via the interplay between apoptosis and autophagy: implications for blood-brain barrier integrity in stroke. *Transl Stroke Res.* 2020;11(2):267-87. <https://doi.org/10.1007/s12975-019-00711-0>
2. Zhang Z, Cho S, Rehni AK, Quero HN, Dave KR, Zhao W. Automated assessment of hematoma volume of rodents subjected to experimental intracerebral hemorrhagic stroke by bayes segmentation approach. *Transl Stroke Res.* 2020;11(4):789-98. <https://doi.org/10.1007/s12975-019-00754-3>
3. Gross BA, Jankowitz BT, Friedlander RM. Cerebral intraparenchymal hemorrhage: a review. *JAMA.* 2019;321(13):1295-303. <https://doi.org/10.1001/jama.2019.2413>.
4. Chen J, Zhu J, He J, Wang Y, Chen L, Zhang C, Zhou J, Yang L. Ultra-early microsurgical treatment within 24 h of SAH improves prognosis of poor-grade aneurysm combined with intracerebral hematoma. *Oncol Lett.* 2016;11(5):3173-8. <https://doi.org/10.3892/ol.2016.4327>
5. Hanley DF, Thompson RE, Rosenblum M, Yenokyan G, Lane K, McBee N, Mayo SW, Bistran-Hall AJ, Gandhi D, Mould WA, Ullman N, Ali H, Carhuapoma JR, Kase CS, Lees KR, Dawson J, Wilson A, Betz JF, Sugar EA, Hao Y, Avadhani R, Caron JL, Harrigan MR, Carlson AP, Bulters D, LeDoux D, Huang J, Cobb C, Gupta G, Kitagawa R, Chicoine MR, Patel H, Dodd R, Camarata PJ, Wolfe S, Stadnik A, Money PL, Mitchell P, Sarabia R, Harnof S, Barzo P, Unterberg A, Teitelbaum JS, Wang W, Anderson CS, Mendelow AD, Gregson B, Janis S, Vespa P, Ziai W, Zuccarello M, Awad IA. Efficacy and safety of minimally invasive surgery with thrombolysis in intracerebral haemorrhage evacuation (MISTIE III): a randomised, controlled, open-label, blinded endpoint phase 3 trial. *Lancet.* 2019;393(10175):1021-32. [https://doi.org/10.1016/s0140-6736\(19\)30195-3](https://doi.org/10.1016/s0140-6736(19)30195-3)
6. Chen J, Wang Y, Wu J, Yang J, Li M, Chen Q. The potential value of targeting ferroptosis in early brain injury after acute CNS disease. *Front Mol Neurosci.* 2020;13:110. <https://doi.org/10.3389/fnmol.2020.00110>
7. Adeoye O, Broderick JP. Advances in the management of intracerebral hemorrhage. *Nat Rev Neurol.* 2010;6(11):593-601. <https://doi.org/10.1038/nrneurol.2010.146>
8. Wu X, Luo J, Liu H, Cui W, Guo K, Zhao L, Bai H, Guo W, Guo H, Feng D, Qu Y. Recombinant adiponectin peptide ameliorates brain injury following intracerebral hemorrhage by suppressing astrocyte-derived inflammation via the inhibition of drp1-mediated mitochondrial fission. *Transl Stroke Res.* 2020;11(5):924-39. <https://doi.org/10.1007/s12975-019-00768-x>
9. Mendelow AD, Gregson BA, Rowan EN, Murray GD, Gholkar A, Mitchell PM. Early surgery versus initial conservative treatment in patients with spontaneous supratentorial lobar intracerebral haematomas (STICH II): a randomised trial. *Lancet.* 2013;382(9890):397-408. [https://doi.org/10.1016/s0140-6736\(13\)60986-1](https://doi.org/10.1016/s0140-6736(13)60986-1)
10. Bao WD, Zhou XT, Zhou LT, Wang F, Yin X, Lu Y, Zhu LQ, Liu D. Targeting miR-124/Ferroportin signaling ameliorated neuronal cell death through inhibiting apoptosis and ferroptosis in aged intracerebral hemorrhage murine model. *Aging Cell.* 2020;19(11):e13235. <https://doi.org/10.1111/acel.13235>

11. Chen JH, Yang LK, Chen L, Wang YH, Wu Y, Jiang BJ, Zhu J, Li PP. Atorvastatin ameliorates early brain injury after subarachnoid hemorrhage via inhibition of AQP4 expression in rabbits. *Int J Mol Med*. 2016;37(4):1059-66. <https://doi.org/10.3892/ijmm.2016.2506>
12. Gautam J, Xu L, Nirwane A, Nguyen B, Yao Y. Loss of mural cell-derived laminin aggravates hemorrhagic brain injury. *J Neuroinflammation*. 2020;17(1):103. <https://doi.org/10.1186/s12974-020-01788-3>
13. Li H, Lu C, Yao W, Xu L, Zhou J, Zheng B. Dexmedetomidine inhibits inflammatory response and autophagy through the circLrp1b/miR-27a-3p/Dram2 pathway in a rat model of traumatic brain injury. *Aging (Albany NY)*. 2020;12(21):21687-705. <https://doi.org/10.18632/aging.103975>
14. Wang Y, Zhao M, Shang L, Zhang Y, Huang C, He Z, Luo M, Wu B, Song P, Wang M, Duan F. Homer1a protects against neuronal injury via PI3K/AKT/mTOR signaling pathway. *Int J Neurosci*. 2020;130(6):621-30. <https://doi.org/10.1080/00207454.2019.1702535>
15. Zrzavy T, Schwaiger C, Wimmer I, Berger T, Bauer J, Butovsky O, Schwab JM, Lassmann H, Höftberger R. Acute and non-resolving inflammation associate with oxidative injury after human spinal cord injury. *Brain*. 2021;144(1):144-61. <https://doi.org/10.1093/brain/awaa360>
16. Wang C, Shao C, Zhang L, Siedlak SL, Meabon JS, Peskind ER, Lu Y, Wang W, Perry G, Cook DG, Zhu X. Oxidative stress signaling in blast TBI-induced Tau phosphorylation. *Antioxidants (Basel)*. 2021;10(6):955. <https://doi.org/10.3390/antiox10060955>
17. Montivero AJ, Gherzi MS, Silvero CM, Artur de la Villarmois E, Catalan-Figueroa J, Herrera M, Becerra MC, Hereñú CB, Pérez MF. Early IGF-1 gene therapy prevented oxidative stress and cognitive deficits induced by traumatic brain injury. *Front Pharmacol*. 2021;12:672392. <https://doi.org/10.3389/fphar.2021.672392>
18. Nakanishi K, Takeda S, Sakamoto A, Kitamura A. Effects of ulinastatin treatment on the cardiopulmonary bypass-induced hemodynamic instability and pulmonary dysfunction. *Crit Care Med*. 2006;34(5):1351-7. <https://doi.org/10.1097/01.Ccm.0000215110.55899.Ae>
19. Liu T, Liao XZ, Zhou MT. Ulinastatin alleviates traumatic brain injury by reducing endothelin-1. *Transl Neurosci*. 2021;12(1):1-8. <https://doi.org/10.1515/tnsci-2021-0001>
20. Ji J, Hong X, Su L, Liu Z. Proteomic identification of hippocalcin and its protective role in heatstroke-induced hypothalamic injury in mice. *J Cell Physiol*. 2019;234(4):3775-89. <https://doi.org/10.1002/jcp.27143>
21. He QL, Zhong F, Ye F, Wei M, Liu WF, Li MN, Li QB, Huang WQ, Sun LB, Shu HH. Does intraoperative ulinastatin improve postoperative clinical outcomes in patients undergoing cardiac surgery: a meta-analysis of randomized controlled trials. *Biomed Res Int*. 2014;2014:630835. <https://doi.org/10.1155/2014/630835>
22. Cui L, Cao W, Xia Y, Li X. Ulinastatin alleviates cerebral ischemia-reperfusion injury in rats by activating the Nrf-2/HO-1 signaling pathway. *Ann Transl Med*. 2020;8(18):1136. <https://doi.org/10.21037/atm-20-5115>
23. Li XF, Zhang XJ, Zhang C, Wang LN, Li YR, Zhang Y, He TT, Zhu XY, Cui LL, Gao BL. Ulinastatin protects brain against cerebral ischemia/reperfusion injury through inhibiting MMP-9 and alleviating loss of ZO-1 and occludin proteins in mice. *Exp Neurol*. 2018;302:68-74. <https://doi.org/10.1016/j.expneurol.2017.12.016>
24. Liu M, Shen J, Zou F, Zhao Y, Li B, Fan M. Effect of ulinastatin on the permeability of the blood-brain barrier on rats with global cerebral ischemia/reperfusion injury as assessed by MRI. *Biomed Pharmacother*. 2017;85:412-7. <https://doi.org/10.1016/j.biopha.2016.11.044>
25. Vandenabeele P, Galluzzi L, Vanden Berghe T, Kroemer G. Molecular mechanisms of necroptosis: an ordered cellular explosion. *Nat Rev Mol Cell Biol*. 2010;11(10):700-14. <https://doi.org/10.1038/nrm2970>
26. Chen T, Yang LK, Zhu J, Hang CH, Wang YH. The AMPAR antagonist perampanel regulates neuronal necroptosis via Akt/GSK3 β signaling after acute traumatic injury in cortical neurons. *CNS Neurol Disord Drug Targets*. 2021;20(3):266-72. <https://doi.org/10.2174/1871527319666201001110937>
27. Chen T, Zhu J, Wang YH, Hang CH. Arc silence aggravates traumatic neuronal injury via mGluR1-mediated ER stress and necroptosis. *Cell Death Dis*. 2020;11(1):4. <https://doi.org/10.1038/s41419-019-2198-5>

28. Bao Z, Fan L, Zhao L, Xu X, Liu Y, Chao H, Liu N, You Y, Liu Y, Wang X, Ji J. Silencing of A20 aggravates neuronal death and inflammation after traumatic brain injury: a potential trigger of necroptosis. *Front Mol Neurosci.* 2019;12:222. <https://doi.org/10.3389/fnmol.2019.00222>
29. Laird MD, Wakade C, Alleyne CH, Jr., Dhandapani KM. Hemin-induced necroptosis involves glutathione depletion in mouse astrocytes. *Free Radic Biol Med.* 2008;45(8):1103-14. <https://doi.org/10.1016/j.freeradbiomed.2008.07.003>
30. Shen H, Liu C, Zhang D, Yao X, Zhang K, Li H, Chen G. Role for RIP1 in mediating necroptosis in experimental intracerebral hemorrhage model both in vivo and in vitro. *Cell Death Dis.* 2017;8(3):e2641. <https://doi.org/10.1038/cddis.2017.58>
31. Zhang Y, Li M, Li X, Zhang H, Wang L, Wu X, Zhang H, Luo Y. Catalytically inactive RIP1 and RIP3 deficiency protect against acute ischemic stroke by inhibiting necroptosis and neuroinflammation. *Cell Death Dis.* 2020;11(7):565. <https://doi.org/10.1038/s41419-020-02770-w>
32. Yuan J, Amin P, Ofengeim D. Necroptosis and RIPK1-mediated neuroinflammation in CNS diseases. *Nat Rev Neurosci.* 2019;20(1):19-33. <https://doi.org/10.1038/s41583-018-0093-1>
33. Linkermann A, Green DR. Necroptosis. *N Engl J Med.* 2014;370(5):455-65. <https://doi.org/10.1056/NEJMra1310050>
34. Jiayong Z, Shengchen W, Xiaofang H, Gang S, Shiwen X. The antagonistic effect of selenium on lead-induced necroptosis via MAPK/NF- κ B pathway and HSPs activation in the chicken spleen. *Ecotoxicol Environ Saf.* 2020;204:111049. <https://doi.org/10.1016/j.ecoenv.2020.111049>
35. Yu Z, Jiang N, Su W, Zhuo Y. Necroptosis: a novel pathway in neuroinflammation. *Front Pharmacol.* 2021;12:701564. <https://doi.org/10.3389/fphar.2021.701564>
36. Deng S, Sherchan P, Jin P, Huang L, Travis Z, Zhang JH, Gong Y, Tang J. Recombinant CCL17 enhances hematoma resolution and activation of CCR4/ERK/Nrf2/CD163 signaling pathway after intracerebral hemorrhage in mice. *Neurotherapeutics.* 2020;17(4):1940-53. <https://doi.org/10.1007/s13311-020-00908-4>
37. Tang C, Shan Y, Hu Y, Fang Z, Tong Y, Chen M, Wei X, Fu X, Xu X. FGF2 Attenuates neural cell death via suppressing autophagy after rat mild traumatic brain injury. *Stem Cells Int.* 2017;2017:2923182. <https://doi.org/10.1155/2017/2923182>
38. Chen JH, Wu T, Xia WY, Shi ZH, Zhang CL, Chen L, Chen QX, Wang YH. An early neuroprotective effect of atorvastatin against subarachnoid hemorrhage. *Neural Regen Res.* 2020;15(10):1947-54. <https://doi.org/10.4103/1673-5374.280326>
39. Chen J, Xuan Y, Chen Y, Wu T, Chen L, Guan H, Yang S, He J, Shi D, Wang Y. Netrin-1 alleviates subarachnoid haemorrhage-induced brain injury via the PPAR gamma/NF-KB signalling pathway. *J Cell Mol Med.* 2019;23(3):2256-62. <https://doi.org/10.1111/jcmm.14105>
40. Chen J, Zhang C, Yan T, Yang L, Wang Y, Shi Z, Li M, Chen Q. Atorvastatin ameliorates early brain injury after subarachnoid hemorrhage via inhibition of pyroptosis and neuroinflammation. *J Cell Physiol.* 2021;236(10):6920-31 <https://doi.org/10.1002/jcp.30351>
41. Li G, Dong Y, Liu D, Zou Z, Hao G, Gao X, Pan P, Liang G. NEK7 Coordinates rapid neuroinflammation after subarachnoid hemorrhage in mice. *Front Neurol.* 2020;11:551. <https://doi.org/10.3389/fneur.2020.00551>
42. Chen J-H, Wu T, Yang L-K, Chen L, Zhu J, Li P-P, Hu X, Wang Y-H. Protective effects of atorvastatin on cerebral vessel autoregulation in an experimental rabbit model of subarachnoid hemorrhage. *Mol Med Rep.* 2018;17(1):1651-9. <https://doi.org/10.3892/mmr.2017.8074>
43. Liu L, Zhao L, Liu Y, Yu X, Qiao X. Rutin ameliorates cadmium-induced necroptosis in the chicken liver via inhibiting oxidative stress and MAPK/NF- κ B pathway. *Biol Trace Elem Res.* 2022 Apr;200(4):1799-810. <https://doi.org/10.1007/s12011-021-02764-5>
44. Chi Q, Wang D, Hu X, Li S, Li S. Hydrogen sulfide gas exposure induces necroptosis and promotes inflammation through the MAPK/NF- κ B pathway in broiler spleen. *Oxid Med Cell Longev.* 2019;2019:8061823. <https://doi.org/10.1155/2019/8061823>
45. Liu S, Xu J, Gao Y, Shen P, Xia S, Li Z, Zhang M. Multi-organ protection of ulinastatin in traumatic cardiac arrest

model. *World J Emerg Surg.* 2018;13:51. <https://doi.org/10.1186/s13017-018-0212-3>

46. Karnad DR, Bhadade R, Verma PK, Moulick ND, Daga MK, Chafekar ND, Iyer S. Intravenous administration of ulinastatin (human urinary trypsin inhibitor) in severe sepsis: a multicenter randomized controlled study. *Intensive Care Med.* 2014;40(6):830-8. <https://doi.org/10.1007/s00134-014-3278-8>
47. Lv B, Jiang XM, Wang DW, Chen J, Han DF, Liu XL. Protective effects and mechanisms of action of ulinastatin against cerebral ischemia-reperfusion injury. *Curr Pharm Des.* 2020;26(27):3332-40. <https://doi.org/10.2174/1381612826666200303114955>
48. Cui T, Zhu G. Ulinastatin attenuates brain edema after traumatic brain injury in rats. *Cell Biochem Biophys.* 2015;71(2):595-600. <https://doi.org/10.1007/s12013-014-0239-3>
49. Yang L, Wang Y, Zhang C, Chen T, Cheng H. Perampanel, an AMPAR antagonist, alleviates experimental intracerebral hemorrhage-induced brain injury via necroptosis and neuroinflammation. *Mol Med Rep.* 2021;24(2):544. <https://doi.org/10.3892/mmr.2021.12183>
50. Chang P, Dong W, Zhang M, Wang Z, Wang Y, Wang T, Gao Y, Meng H, Luo B, Luo C, Chen X, Tao L. Anti-necroptosis chemical necrostatin-1 can also suppress apoptotic and autophagic pathway to exert neuroprotective effect in mice intracerebral hemorrhage model. *J Mol Neurosci.* 2014;52(2):242-9. <https://doi.org/10.1007/s12031-013-0132-3>
51. Lule S, Wu L, Sarro-Schwartz A, Edmiston WJ, 3rd, Izzy S, Songtachalert T, Ahn SH, Fernandes ND, Jin G, Chung JY, Balachandran S, Lo EH, Kaplan D, Degtrev A, Whalen MJ. Cell-specific activation of RIPK1 and MLKL after intracerebral hemorrhage in mice. *J Cereb Blood Flow Metab.* 2021;41(7):1623-33. <https://doi.org/10.1177/0271678x20973609>
52. Su X, Wang H, Lin Y, Chen F. RIP1 and RIP3 mediate hemin-induced cell death in HT22 hippocampal neuronal cells. *Neuropsychiatr Dis Treat.* 2018;14:3111-9. <https://doi.org/10.2147/ndt.S181074>
53. Kim YM, Kim HJ, Chang KC. Glycyrrhizin reduces HMGB1 secretion in lipopolysaccharide-activated RAW 264.7 cells and endotoxemic mice by p38/Nrf2-dependent induction of HO-1. *Int Immunopharmacol.* 2015;26(1):112-8. <https://doi.org/10.1016/j.intimp.2015.03.014>
54. Li X, Su L, Zhang X, Zhang C, Wang L, Li Y, Zhang Y, He T, Zhu X, Cui L. Ulinastatin downregulates TLR4 and NF-kB expression and protects mouse brains against ischemia/reperfusion injury. *Neurol Res.* 2017;39(4):367-73. <https://doi.org/10.1080/01616412.2017.1286541>